

LGVTON: A Landmark Guided Approach to Virtual Try-On

Debapriya Roy, Sanchayan Santra, Bhabatosh Chanda

Abstract—We address the problem of image based virtual try-on (VTON), where the goal is to synthesize an image of a person wearing the cloth of a model. An essential requirement for generating a perceptually convincing VTON result is preserving the characteristics of the cloth and the person. Keeping this in mind we propose *LGVTON*, a novel self-supervised landmark guided approach to image based virtual try-on. The incorporation of self-supervision tackles the problem of lack of paired training data in model to person VTON scenario. *LGVTON* uses two types of landmarks to warp the model cloth according to the shape and pose of the person, one, human landmarks, the locations of anatomical keypoints of human, two, fashion landmarks, the structural keypoints of cloth. We introduce an unique way of using landmarks for warping which is more efficient and effective compared to existing warping based methods in current problem scenario. In addition to that, to make the method robust in cases of noisy landmark estimates that causes inaccurate warping, we propose a mask generator module that attempts to predict the true segmentation mask of the model cloth on the person, which in turn guides our image synthesizer module in tackling warping issues. Experimental results show the effectiveness of our method in comparison to the state-of-the-art VTON methods.

I. INTRODUCTION

In the recent years, popularity of online shopping of fashion items has increased to a great extent all over the world. This has put forth the concept of virtual try-on (VTON) that allows a person to try a cloth virtually. The existing VTON systems based on 3D body shape of the person [[1], [2]] produce enhanced VTON experience but incur significant cost of computation and require expensive devices to capture the 3D data.



Fig. 1: Illustrating the objective of the present work. Given model and person images, the proposed method generates the image of the person wearing the model's cloth.

Recent methods of VTON [[3], [4], [5], [6], [7], [8], [9], [10]] have explored image based approach to solve the problem. Compared to the 3D model based methods, image based VTON systems are much less resource intensive with variety of scopes.

D. Roy, S. Santra and B. Chanda are with Indian Statistical Institute, Kolkata.
E-mail: {debapriyakundu1, sanchayan.santra}@gmail.com, chanda@isical.ac.in.
This paper contains a supplementary material.

However, generating a perceptually convincing image without 3D shape of the person and model is quite challenging.

In modern era plenty of images of persons or models are available over social media or online apparel shopping websites. However, most of the image based VTON methods [3], [4], [5], [6], [7], [8], [9] need separate cloth image as input, which is rarely available. So VTON systems with only model and person images as input would increase the scope of image based VTON enormously. Our method belongs to this group.

Prior to our work, M2E-TON [10] attempted this approach. It includes a pose alignment network to align the model image on to the pose of the person using their dense pose representations [11]. The aligned model image is then passed through a texture refinement network that enhances the textures and colours of the image. This is followed by a fitting network that merges the aligned cloth area of the refined model image with the person image to generate the final output. Fig. 2 shows some results generated by M2E-TON. By careful analysis of the results we find a few limitations: (1) The textures and colours are not preserved well in the final results (1st and 3rd row), (2) [10] cannot distinguish between head pattern printed on cloth and actual head of human (2nd row), (3) [10] may not transfer the true fitting of the cloth, for example, in the 1st row, the sleeves of the shirt are loosely fitted to the model while in result those are tightly fitted, and (4) background of the person image may change as seen in the 3rd case, where a shadow is generated in the background. Moreover, there may be change in image brightness as observed in all the resultant images the face looks brighter than the original. In addition to M2E-TON we also consider two benchmark VTON methods: VITON [4] and CP-VTON [5]. Their objective differs from ours in a sense that instead of model image those methods require image of the desired cloth separately as input, which is seldom available. Both of them initially do the warping of the cloth followed by merging it with the target person. VITON is not able to keep the characteristics of the cloth well in the final output as pointed out in [5]. On the other hand, though CP-VTON tried to address this issue but its geometric matching module often falls short of generating realistic warping. Moreover, both of them sometimes fail to preserve the other parts of clothing of person.

To address these challenges we propose a novel approach for VTON, namely *LGVTON* (A Landmark Guided Approach to VTON) that introduces an unique way of leveraging human and fashion landmarks in the context of VTON and also proposes a method to address warping issues. An overview of it is given in Fig. 4. The concept is implemented by means of three major algorithmic steps, such as pose guided cloth warping, mask



Fig. 2: Visual comparison of results of LGVTON (our method) with that of M2E-TON. Zoom-in for details.

generation and image synthesizing.

Each of these steps is accomplished by one module namely Pose Guided Warping Module (PGWM), Mask Generator Module (MGM), Image Synthesizer Module (ISM) respectively.

Pose Guided Warping Module (PGWM) - it aligns the model cloth to the body shape and pose of the person using human and fashion landmarks, *Mask Generator Module (MGM)* - it attempts to predicts the true segmentation mask of the model clothing on the person that helps the next module to tackle any shortcomings in the aligned cloth that occurred due to error in estimation of landmarks in PGWM, *Image Synthesizer Module (ISM)* - it combines the warped clothing with the person image to generate the final VTON output. ISM generates a combination mask that helps in preserving the characteristics of the warped clothing and the person image and leads to an enhanced VTON output.

It is observed experimentally that LGVTON achieves promising performance both qualitatively and quantitatively in comparison to the state of the art VTON methods. Similar to VITON and CP-VTON our work focuses on upper body cloths only. The contributions of the proposed method may be summarized as follows.

- 1) We show the effectiveness of fashion and human landmarks for aligning the model cloth according to the shape of the person, while also propose a method for estimating fashion landmarks of the target warp of the model cloth. Unlike M2E-TON that aligns the whole model image we are aligning the model cloth only which is more time efficient. In contrast to the warping method of CP-VTON our method ensures the target landmark locations are preserved after warping, which results in more realistic warping.
- 2) Both CP-VTON, VITON generates the target warp and combines it with the person but does not handle in case there is any existing warping issue. We address this using our mask generator and image synthesizer module.
- 3) Our image synthesizer generates the final virtual try-on result in a way that not only keeps the characteristics of the cloth but also keeps the details of the person very well. This addresses the problem of loss of cloth details of the target person that sometimes occur in the results of VTON, CP-VTON, M2E-TON. This in effect results in better VTON output compared to existing methods.



Fig. 3: Demonstration of two types of landmarks used by LGVTON.

- 4) Ideally, supervised training of model to person virtual try-on system, require images of model and person wearing the same cloth. However, such a data pair is hard to get. So we propose an self-supervised training approach, which implies during training each pair of model and person image contains same images.

Rest of the paper is organised as follows. The existing works related to VTON is discussed in Sec. II. Our entire approach is explained in detail in sec. III. Sec. IV presents the qualitative and quantitative results on benchmark data and discussion thereof. In sec. V, a systematic ablation study is described, and finally we conclude in sec. VI.

II. RELATED WORKS

A. Human parsing and pose understanding

Understanding human in images generally involves finding their body, estimating human pose [12] and parsing [13], [14]. Pose estimation is the problem of localizing anatomical keypoints of human, called *human landmarks*. Whereas body parsing and cloth parsing refers to the segmentation of human image into multiple parts with fine-grained semantics. These has been used in many tasks such as - human behaviour analysis [15], person re-identification [16]. Cao et al. [12] proposed a part affinity field (PAF) based method for localizing the human landmarks, where PAF is a non-parametric representation that learns to associate body parts of the person in the image. Present work uses the method presented in [12] for localizing the human landmarks of the model and the person. This facilitates aligning the model cloth efficiently that is extracted from the model image using [14], which is a human parsing approach that employs structural information in parsing scenario. Densepose [11] maps the human pixels of an image to the 3D surface of the human body. We utilize it to obtain structural information of the person which plays critical role in our synthesizer module.

B. Visual fashion analysis

Due to many human-centric applications, visual fashion analysis has attracted a wide attention over last few years. Localizing fashion landmarks [17], [18], clothing category classification [18] are some of the key issues addressed in this domain.

C. Virtual try-on (VTON)

In the existing approaches the virtual try-on has been attempted either using 3D body modelling based methods

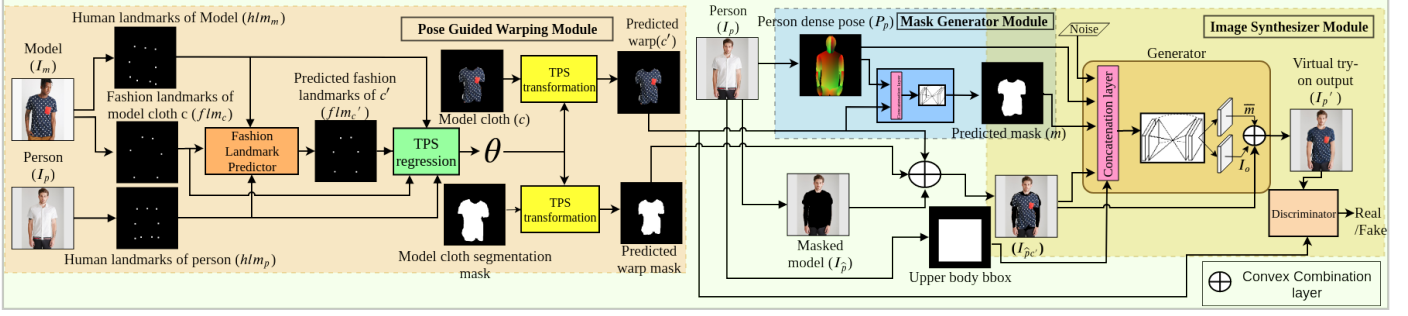


Fig. 4: Block diagram depicting workflow of LGVTON. [Best viewed in electronic version.]

[19], [1] or image based methods [20], [21], [3], [4], [5], [10], [6], [7], [8], [9]. In [1], the proposed system tries to capture high resolution 3d scan of a person, extract his/her clothing followed by re-targeting it on a new person. On the other hand, Sekine et al. [2] proposed to estimate the 3D shape of a person and fit a 2D image onto it virtually.

In [20] the authors propose a conditional GAN [22] based two-stage pipeline to swap the clothing between a pair of person images. [21] transfers the appearance from the source person image onto the target person image while preserving the clothing segmentation layout of the source person. The objective of [20], [21] is to transfer the complete appearance, while we are interested in transferring a desired clothing only. CAGAN [3] trained a conditional GAN with cycle consistency loss to learn the relation between a cloth image and its appearance rendered on a human but training of it requires images of same person wearing different cloths in same pose, which is rarely available. VITON [4] uses a coarse-to-fine framework for VTION. But lacks keeping the details of the cloth well in the result. On the other hand, CP-VTON [5] addresses this issue by using mask that helps to retain the characteristics of the cloth. M2E-TON [10] transfers clothing from model to person. It aligns the model image to the shape and pose of the person using their dense pose [11] representations. The texture of transformed model image is refined by a texture refinement network. The aligned model image is finally merged with the person image using a fitting network. All the above mentioned VTION methods except M2E-TON require the image of the clothing separately which is rarely available. So like M2E-TON we also address the problem of transferring cloth from model to person which is more pragmatic.

III. METHODOLOGY

We propose a method, called LGVTION, for virtually trying cloths from a model image onto a person image. Given a model image I_m and a person image I_p it generates a new image I_p' of the person wearing the clothing of I_m . As shown in Fig. 4 LGVTION proceeds in the following way, first it attempts to compute the target warp of the model cloth c which is done by our Pose guided Warping Module (PGWM). It works in two steps - first, predicting the fashion landmarks of the target warp of c , second, transforming c to c' based on the landmark correspondences. Then a segmentation mask corresponding to the true warp of the model cloth for the person is predicted

by our Mask generator Module (MGM). This is followed by synthesizing the final virtual try-on output using our Image Synthesizer Module (ISM). Note that by landmarks we refer to the locations of landmarks. We use estimation and prediction interchangeably in describing PGWM.

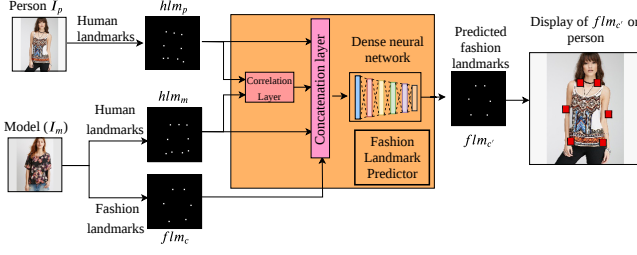
A. Finding the target warp of the model cloth

This section elaborates our Pose Guided Warping Module (PGWM) which computes a thin plate spline (TPS) transformation function $f(\cdot; \theta)$ to warp c to its target warp c' . c is obtained from I_m using the human parsing network proposed by [14]. Generation of c' involves two steps discussed below.

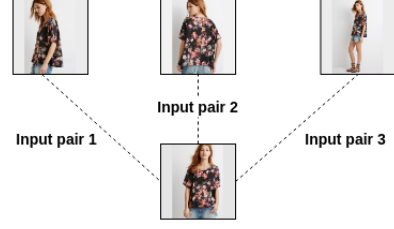
1) *Estimating fashion landmarks of the target warp cloth:* Our method of computing c' requires estimation of its fashion landmarks and human landmarks of I_p . We extract human landmarks using [12]. As computing the deformation of a non-rigid object such as cloth (e.g., c to c') is very challenging, and achieving good warping usually requires many landmarks. So along with human landmarks we consider fashion landmarks as well, the necessity of it is elaborated in Sec. V. As this work is targeted to upper body cloths only, so for warping we use only upper body human landmarks which in total is 9 and fashion landmarks corresponding to upper body cloths which in total is 6 (refer to Fig. 3).

We propose a fashion landmark predictor network \mathcal{F} that predicts the fashion landmarks $flm_{c'}$ of c' (refer to Fig. 5a). The inputs to this network are human landmarks of model hlm_m , that of person hlm_p and fashion landmarks flm_c of model cloth c .

Correlation between the human landmarks of the model and that of the person plays significant role in estimating $flm_{c'}$. We incorporate this observation in \mathcal{F} by introducing a correlation layer with inputs hlm_m and hlm_p . To establish the efficacy and usefulness of correlation layer we have performed an ablation study on it in Sec. V. The loss function used to train \mathcal{F} is defined as: $Loss = \|N(hlm_m, flm_c, hlm_p) - flm_{c'}\|_2^2$. Training this network requires adequate number of paired data, i.e., human and fashion landmarks of two persons wearing same cloths in any arbitrary pose, which is not available. However, images of same person wearing same cloth, but in different poses are available. An example of such sample is shown in Fig. 5b. We leverage this data to train \mathcal{F} , where one of them is considered model and the other as target person. Each data pair is considered twice alternating the role of each image between model and image. Some results of \mathcal{F} are shown in Fig. 6.



(a) Block diagram of fashion landmark predictor network (F).



(b) Sample training data pairs.

Fig. 5: Fashion landmark predictor in Pose guided warping module (PGWM).



Fig. 6: Results of the two steps of PGWM and final output of LGVTION.

2) *Computing the target warp*: Based on the correspondences between the two sets of landmarks $\{flm_c, hlm_m\}$ and $\{flm_c', hlm_p\}$ we aim to transform c to its target warp c' . Hence formally we may say, given a set of pair of source and target landmarks $\{(\mathbf{r}_j, \mathbf{t}_j); j = 1, \dots, N\}$ our objective is to find a smooth function $f(\cdot)$ satisfying the interpolation condition,

$$f(\mathbf{r}_j) = \mathbf{t}_j. \quad (1)$$

Then we apply that $f(\cdot)$ on the grid of c to get c' . Now deformation of non-rigid object such as cloth should be smooth. Considering this, we choose $f(\cdot)$ to be a thin plate spline (TPS) transform [23], which is a widely used transform representing coordinate mappings and involves a penalty term to impose smoothness [a detailed study on TPS is given in the supplementary material].

Now as we are dealing with only estimates of the true landmark locations which may be noisy so instead of exact interpolation our goal reduces to approximation. This is accomplished in TPS transform by minimizing the following objective functional [[24],[25]],

$$H[f] = \sum_{j=1}^N \|f(\mathbf{r}_j) - \mathbf{t}_j\|_2^2 + \lambda \int \int [f_{xx}^2 + 2f_{xy}^2 + f_{yy}^2] dx dy, \quad (2)$$

where λ is a regularization parameter which is a positive scalar and f_{xx}, f_{xy}, f_{yy} are second-order gradients of $f(\cdot)$ as $\mathbf{r} \equiv (r^x, r^y)$ and $\mathbf{t} \equiv (t^x, t^y)$.

In our problem we have $N = 15$ landmarks (9 human landmarks and 6 fashion landmarks). The source set of landmarks $\{\mathbf{r}_j; j = 1, \dots, N\}$ are $\{flm_c, hlm_m\}$ and the target

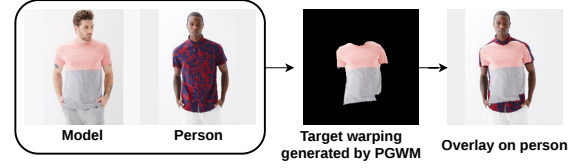


Fig. 7: Demonstration of warping fault. The target warping generated by the PGWM is not completely accurate as it is observable when overlaid on the person image. This is due to improper estimation of locations of fashion landmarks in the PGWM. The warped cloth does not fit properly in the areas near collar and hands.

set of landmarks $\{\mathbf{t}_j; j = 1, \dots, N\}$ are $\{flm_c', hlm_p\}$. We take $\lambda = 0.01$, which we observed experimentally to be more effective. Some target warps generated by PGWM are shown in Fig. 6.

B. Generating Mask for Virtual Clothing

The problem of working with estimated landmarks is that noisy estimates will result in inaccurate warping which we refer as warping faults, shown in Fig. 7.

To deal with this issues our next module *mask generator module* (MGM) [shown in Fig. 8] comes into play which aims to predict the segmentation mask denoting the region of the virtually tried clothing in the VTION output. This mask guides the next stage of our proposed system to handle the warping faults. MGM takes c' (obtained by TPS as described in the previous subsection) and densepose P_p of the person and aims to predict the true mask m of refined c' , where refined c' refers to the correct target warp of c . MGM learns the structural feature of the cloth image of the model and associates it with the densepose of the person to predict m , where a densepose prediction contains 24 part labels of human, where each part has UV parametric values of the body surface. For training

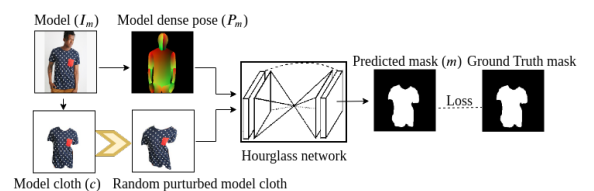


Fig. 8: Mask generator module (training scenario). [Best viewed in electronic version.]

MGM, we generate a random warp of c , say, \hat{c} in the following way. We perturb function landmarks flm_c of the model by adding random noise $\mathcal{N}(0, 0.001)$ to it and denote it by $flm_{\hat{c}}$. A transformation based on TPS between flm_c and $flm_{\hat{c}}$ is used to warp c to \hat{c} . Now to train MGM, we provide an input pair $\{\hat{c}, P_m\}$, where P_m is the densepose representation of the model. The groundtruth of the result for this pair is the mask of c . Several \hat{c} is generated for each c to train this module. Multiple warps of same cloth makes the network learn to extract features from cloth which does not change with landmark perturbations. This enables the network to predict the true segmentation mask of model cloth on the person, which is the objective of MGM.

C. Synthesizing VTON image

This section describes our final module *image synthesizer module* (ISM) [shown in Fig. 4]] that combines c' and I_p to generate the final virtual try-on output I_p' . ISM is based on conditional generative adversarial network (cGAN), which is an extension of GAN [26] where both the generator and discriminator are conditioned on some extra information.

Instead of providing I_p and c' separately to ISM we make a combined input by manipulating I_p to generate $I_{\hat{p}}$ which is the image of the person with pixel values set to zero in the upper body area and then combining it with c' . $I_{\hat{p}}$ is computed as: $I_{\hat{p}} = I_p \times (m_{p_u} || m_{p_c})$, where m_{p_u} denotes the segmentation mask of the hands and torso of I_p , obtained from the densepose [11] representation of I_p and m_{p_c} denotes the segmentation mask of the upper body cloth of I_p obtained from its human parsing [14]. Due to the self-supervised training of ISM, during training ISM learns to synthesize the image of the model wearing his own cloth, causing m_{p_c} and m to be same. This causes network to fail for test cases as then m_{p_c} and m are different. To overcome this issue m_{p_c} is dilated with a kernel of random size during training. This induces a difference between m_{p_c} and m . Finally c' is combined with $I_{\hat{p}}$ to get the final input $I_{\hat{p}c'}$.

Our self-supervised training methodology causes c' to be same as c during training, so there is no possibility of warping fault. However, to make our network robust to warping faults, which may occur during testing phase, we induce warping fault artificially in c' during training. To do that, we perturb flm_c to flm'_c by adding random values from $\mathcal{N}(0, 0.001)$, and warp c using a TPS transform between flm_c and flm'_c . The list of inputs to ISM is as follows.

- 1) The generated target cloth mask m from MGM.
- 2) Image of person $I_{\hat{p}}$ with pixel values set to zero in the upper body area including the upper body cloth and the predicted warped cloth c' from PGWM combined with it. This is denoted by $I_{\hat{p}c'}$.
- 3) Upper body bounding box of I_p , which is computed from the upper body segments of the human parsing.
- 4) Dense pose P_p of I_p .
- 5) random noise \mathbf{z} sampled from a input noise distribution p_z required to train cGAN.

ISM when trained without m generates image artifacts, as shown in Fig. 12(h). This is due to the huge diversity in the

types of cloth designs, which confuses the cGAN to distinguish an warping fault from a cloth design. Whereas in presence of m , ISM is able to tackle it as observed Fig. 12(j). This is further discussed in detail in Sec. V.

The objective of cGAN may be expressed as

$$L_{cGAN}(G, D) = \mathbb{E}_{\mathbf{x} \sim p_{data}} [\log D(\mathbf{x}|\mathbf{y})] + \mathbb{E}_{\mathbf{z} \sim p_z} [\log(1 - D(G(\mathbf{z}|\mathbf{y})))] \quad (3)$$

where the generator G learns a distribution p_g over data \mathbf{x} . It builds a mapping function from a prior noise distribution p_z with a conditional information \mathbf{y} to the data space. While the discriminator D represents the probability of \mathbf{x} given \mathbf{y} , to be coming from the training data rather than the generator distribution p_g [22]. cGAN is trained to minimize an objective L_{cGAN} against an adversarial D that tries to maximize it. The optimum G denoted by G^* is

$$G^* = \arg \min_G \arg \max_D L_{cGAN}(G, D). \quad (4)$$

In our model c' is the condition given to both G and D .

G is a CNN, containing a hourglass network [27], followed by two parallel convolution layers, giving activation I_o , an intermediate VTON output and \tilde{m} , a mask. The last layer of G is a convex combination layer that combines I_o and $I_{\hat{p}c'}$ using \tilde{m} . This is formulated as: $O = \tilde{m} \times I_o + (1 - \tilde{m}) \times I_{\hat{p}c'}$. ISM learns the mask \tilde{m} in unsupervised way (since we do not have any ground truth for this) and \tilde{m} plays a key role to obtain enhanced output in our method. Generally, the averaging tendency of convolution operation causes the loss of fine details in the image. Having this mask helps the network to avoid such loss due to convolution. This can be validated from Fig. 9 which shows that our result retains cloth, person and background details better in comparison to the results of the other methods.

D is a patchGAN discriminator [28]. Instead of classifying the whole image as real or fake, it classifies each patch of the image, where the patch size is much smaller than the input image size. Hence pixels separated by more than a patch diameter gets modelled independently. This makes it work like a texture/style loss as discussed in [28], which helps to keep better texture in the final output image. Existing works have shown the efficacy of patchGAN [28],[29] in image based problems.

It has been experimentally observed by different past works on conditional GAN [30],[29] that having other loss functions, such as perceptual loss [29], along with adversarial loss gives better output. So we incorporate structural dissimilarity (DSSIM) and VGG perceptual loss as additional loss functions in the generator. The inclusion of these additional loss terms keeps the task of discriminator unchanged while the generator in addition to the task of fooling the discriminator has to generate data instances closer (in L2 distance) to the ground truth.

SSIM [31] is an image metric that measures the structural similarity between two images. However in neural network the objective is to minimize the value of the loss function so instead of SSIM we take DSSIM that is related to SSIM the

following way, $DSSIM(\cdot, \cdot) = 1 - SSIM(\cdot, \cdot)$. DSSIM loss for the generator is defined as follows

$$L_{DSSIM}(G) = \mathbb{E}_{\mathbf{z} \sim p_{\mathbf{z}}, \mathbf{x} \sim p_{data}} DSSIM(\mathbf{x}, G(\mathbf{z}|\mathbf{y})) \quad (5)$$

VGG perceptual loss [30] is a $L2$ loss between the features of generated and groundtruth images, obtained from different layers of pre-trained classification network (VGG-19). Instead of exactly matching the pixel values of the generated and groundtruth images this loss matches their feature representations. This encourages the network to produce images which are perceptually similar to their corresponding target images. Formally this loss is defined as

$$L_{VGG}(G) = \mathbb{E}_{\mathbf{z} \sim p_{\mathbf{z}}, \mathbf{x} \sim p_{data}} \left[\sum_{i=1}^{\rho} \frac{1}{C_i H_i W_i} \|(F_i(\mathbf{x}) - F_i(G(\mathbf{z}|\mathbf{y})))\|_2^2 \right], \quad (6)$$

where $F_i(\mathbf{x})$ denotes the activation at the i th layer of VGG-19 for the input image \mathbf{x} . This is a feature map of shape $C_i \times H_i \times W_i$. ρ is the total number of layers of VGG-19 that we are using. We take the features from conv1_2, conv2_2, conv3_2, conv4_3, conv5_1 layers of VGG-19. Hence, our final objective becomes

$$G^{**} = \arg \min_G \arg \max_D (L_{cGAN}(G, D) + L_{DSSIM}(G) + L_{VGG}(G)), \quad (7)$$

IV. EXPERIMENTS

In this section we first introduce the experimental details of the proposed method and then we present a comparative study of LGVTON (our method) with other competitive methods [4],[5],[10],[32] both qualitatively and quantitatively.

A. Dataset

The dataset used in this work is IN-Shop Cloth Retrieval benchmark dataset from deepfashion [33], which contains multiple views of each person (front, side, back and full). It has in total 52,712 images of clothed person. Each image is labelled with bounding box and fashion landmark annotations, which is required for the proposed method. This dataset contains 6 landmarks for upper body cloths and 9 for lower body cloths. However, we are interested in only upper body cloths. So we pick up in total 33,536 images which contains upper body cloth annotations. Before applying our algorithm, we prepare various inputs by some existing methods. These include densepose representation (by [11]), human segmentation (by [14]) and human pose estimates (by [12]) of the images. Due to our self-supervised training strategy our method does not require any train-test split of the dataset. Hence, the entire dataset is used for training. During testing we randomly select a pair of images in front pose.

TABLE I: Quantitative evaluation, each cell represents the value of Frechet Inception Distance (FID) score and Inception score (IS). Method names are specified in the Methods column.

Methods	FID↓	IS↑	SSIM↑
VITON	78.45	2.22 ± 0.103	0.71
CP-VTON	72.95	2.41 ± 0.21	0.72
LGVTON (ours)	56.85	2.71 ± 0.12	0.86

B. Quantitative Comparison

We report the values of three metrics, namely *Inception Score (IS)* [34], *Fréchet Inception Distance (FID)* [35] and *SSIM* [31] for evaluation as well as comparison between our method and other methods.

Inception Score (IS) measures the classifiability and diverseness in the generated image where the generated image is classified using the inception v3 model [36] to predict the class probability. Suppose $p(b|\mathbf{a})$ is the conditional label (b) distribution estimated for image \mathbf{a} using Inception model [36] pre-trained with ImageNet [37], $p(b)$ is the marginal distribution $\int p(b|\mathbf{a} = G(\mathbf{z}))d\mathbf{z}$, then the inception score is calculated by measuring the average Kullback–Leibler (KL) divergence D_{KL} between $p(b|\mathbf{a})$ and $p(b)$. This is formulated as: $\exp(\mathbb{E}_{\mathbf{a} \sim p_g} D_{KL}(p(b|\mathbf{a}) || p(b)))$, where $\mathbf{a} \sim p_g$ denotes an image sampled from p_g . A higher value of IS is better.

Fréchet Inception Distance (FID) is a measure of similarity between two sets of images. It extracts the features embedded in both real and the generated images from a layer of inception v3 model pre-trained with ImageNet. Considering the embedding as continuous multivariate Gaussian, the mean and covariance are estimated for both the generated (μ_g, σ_g) and the real data (μ_r, σ_r). Then the FID is calculated as: $\|\mu_r - \mu_g\|_2^2 + \text{Tr}(\sigma_r + \sigma_g - 2(\sigma_r \sigma_g)^{1/2})$. A lower value of FID is better.

Both IS and FID are popular measures, but as explained in [35], FID is a better measure than IS.

We compare our method with two well-known recently proposed VTON methods CP-VTON [5] and VITON [4]. Although from input perspective these methods are different from ours but since code of M2E-TON is not available so based on its qualitative results a comparative study with it is done in the next section. Unlike ours CP-VTON and VITON require separate cloth image. As the deepfashion dataset does not contain separate cloth image corresponding to each and every model image, so we took a subset of model images from this dataset for which separate cloth images are available, which is in total 517. From this set we randomly selected 8500 pairs of images for our experiment. The values of FID and IS are summarized in Table I. We also report SSIM score in the same Table for the training set of images only, since groundtruth is not available for test set of images. The results demonstrate that our method outperforms both VITON and CP-VTON in terms all the three metrics.

Note that given the model and person images the reported metrics can not measure whether the cloth from model to person has been transferred correctly. Also we don't have any dataset with paired data (different persons wearing same cloth), so comparing with groundtruth is not possible here. Hence, we go for qualitative comparison as adopted in almost all of the existing works [5], [4], [10].



Fig. 9: Qualitative comparison of results of our method with other methods. First five columns are taken from M2E-TON paper.

C. Qualitative Comparison

In this section we present our results and also compare those visually with the results of some base line methods, such as VITON [4], CP-VTON [5], M2E-TON [10] in Fig. 9. CP-VTON and VTON often generates unrealistic warps of the cloth while the amount of distortion is sometimes observed higher in case of CP-VTON. Whereas in our results the predicted warps are much more accurate. This is due to the use of landmarks during warping which imposes restrictions on the deformation and keeps it within desirable limits. We observe that in most of the cases our method retains the desired details of model clothing on the target persons much better than the others. This is due to the combined effect of (i) landmark guided warping of the model clothing, which generates better target warps and (ii) the convex combination layer in the ISM, that helps to retain the details of the warped clothing in the final try-on output. In the result of M2E-TON the colour of the cloth suffers whitening effect and face colour looks brighter. However, no such artifact or photometric change is observed in our result. We also observe that in most of the cases our method preserves the features of the persons better than the others. There is some change in image background colour in the result of M2E-TON (2nd row) also. However, our method does not affect any existing background details.

Human Study: We made a group of 30 volunteers and each person is presented a randomly selected set of 100 results from 8500 total results of each of the 3 methods - VITON, CP-VTON, and LGVTON (ours). A pairwise comparison of results between each of the comparing methods and our method is collected. The results of this study is reported in Table II. We observe that LGVTON performs better in comparison to both CP-VTON and VITON. So both quantitative and qualitative analysis show the effectiveness of our method for generating good quality virtual try-on results.

TABLE II: Human study. Each cell presents the percentage by which LGVTON (our method) is preferred over other method on average.

Methods	Human Study \uparrow
VITON / LGVTON	76.23%
CP-VTON / LGVTON	74.72%

V. ABLATION STUDY

In this section we conduct an in-depth study on the significance of each individual component of LGVTON. Our PGWM uses both human and fashion landmarks for predicting the target warp of the model cloth. Having only human landmarks might serve the purpose but at the cost of increase in the amount of warping fault. We try to control this using fashion landmarks; as having a better warping puts less burden on ISM resulting in a more realistic try-on output. In case of warping fault ISM regenerates lost cloth details (refer to Fig. 12), but obviously this could never be better than the actual cloth details since warping preserves the details like colour, texture, logo etc. of the cloth. Hence a better warped cloth always results in better LGVTON output. Fig. 10 shows two cases portraying the effectiveness of fashion landmarks around collar and hem.



Fig. 10: Role of different fashion landmarks in predicting the target warp of the model cloth in PGWM, (a, b) shows the utility of fashion landmarks around collar and hem respectively. For better understanding of the viewer, instead of showing the generated warped cloth image only, we show the overlay of it on the person image. (1) Person, (2) model, (3) cloth warped using only human landmarks, (4) transformed locations of fashion landmarks of the model cloth, obtained by the corresponding transformation function of (3), (5) cloth warped by PGWM using both human and fashion landmarks, (6) fashion landmarks predicted in PGWM, which is observed to be more accurate than (4). This results in better warping of the model cloth as shown in (5) in comparison to that in (3).

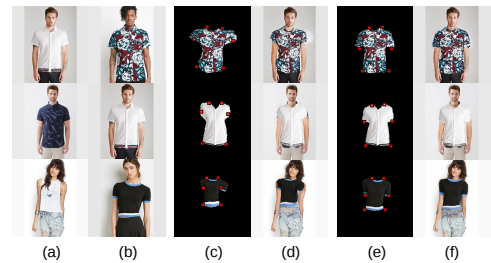


Fig. 11: Study on effectiveness of correlation layer in fashion landmark predictor network \mathcal{F} of PGWP in LGVTON. (a) Person image, (b) Model image, (c, e) predicted locations of fashion landmarks and warp cloths generated by PGWM when \mathcal{F} is trained w/o correlation layer and with correlation layer respectively. (d, f) final VTON result for the warp cloths shown in (c) and (e) respectively. We observe that the results in (f) are better than that in (d), which justifies the potency of correlation layer in PGWM.

We study the effectiveness of correlation layer in fashion landmark predictor network of PGWM (refer to Fig. 11). The presence of correlation layer establishes the relationship between the human poses of the model and the person which in turn assists in predicting better estimates of fashion landmarks of the target warp cloth.

We conduct an experiment to study the usefulness of target mask as input to ISM. The results of this experiment is shown in Fig. 12. For the purpose of understanding the effect of target mask, we train an instance of ISM without providing the target mask as input. Now it is observed w/o target mask the network can not identify warping fault. This can be verified from Fig. 12(h) where the effect of warping fault is propagated to the output. But when a target mask is given as input ISM can identify the areas of warping fault and takes necessary action according to the type of the fault. The reason being, the variety of cloth types makes the network confused to distinguish a fault of warping from a design of cloth, e.g., in the first two rows inappropriate estimation of flm'_c causes the sleeves to be stretched more outwards. While that in Fig. 12(j) is not observed as network removes those areas of extra stretch and replaces with background. In the example of third row Fig. 12(h) the effect of warping fault exposes some body part near right neckline of the person (better viewed when zoomed in), while this gets filled with cloth texture and colour in Fig. 12(j).

We run a comparative study on the effect of different loss functions used to train ISM. Keeping other settings same, we train 3 different instances of ISM with different combinations of loss functions as shown in Fig. 13. As GAN tries to approximate the data distribution so it generates better output than its non-GAN variant [26]. This is observed in the results of LGVTON' and LGVTON'', where due to adversarial loss the blurriness is reduced in LGVTON'' in comparison to the results of LGVTON'. By definition, the objective of perceptual loss is to minimize the distance between the high level features of the result and the ground truth. Since skin colour of person, texture, colour of cloth these are high level features so these details gets reconstructed better in presence of this loss (as observed in the results of LGVTON').

A. Limitations of our method

Our method is sensitive to poor segmentation [14] of the model image as shown in 14(a). We are considering the whole cloth image as a 2d grid, this makes it difficult to model the cross folding of cloth with long sleeves as shown in 14(b). In future we will try to explore more on this direction.

VI. CONCLUSION

This paper presents a self-supervised landmark guided approach to virtual try-on which synthesizes the image of a person wearing a model cloth. Our work is based on the images of model and person without requiring any separate cloth image, which makes it more effective, as having a separate cloth image always is difficult. Our method contains 3 modules. Our first module utilizes the correspondence between the estimated landmark sets of the model and the person to predict the

target warping of the model cloth. Our final module image synthesizer module combines the aligned model cloth and person to synthesize the the final output. A proposed mask generator module guides the synthesizer to tackle in case of noisy estimates of landmarks that lead to incorrect warping. Experimental study demonstrates the ability of our method in generating perceptually convincing virtual try-on outputs.

VII. ACKNOWLEDGEMENT

The authors sincerely thank Aruparna Maity and Dakshya Mishra for their help and also thank Sankha Subhra Mullick for helpful discussion during this work.

REFERENCES

- [1] G. Pons-Moll, S. Pujades, S. Hu, and M. J. Black, "Clothcap: Seamless 4d clothing capture and retargeting," *ACM Transactions on Graphics (TOG)*, vol. 36, no. 4, p. 73, 2017.
- [2] M. Sekine, K. Sugita, F. Perbet, B. Stenger, and M. Nishiyama, "Virtual fitting by single-shot body shape estimation," in *Int. Conf. on 3D Body Scanning Technologies*. Citeseer, 2014, pp. 406–413.
- [3] N. Jettev and U. Bergmann, "The conditional analogy gan: Swapping fashion articles on people images," in *Proceedings of the IEEE International Conference on Computer Vision*, 2017, pp. 2287–2292.
- [4] X. Han, Z. Wu, Z. Wu, R. Yu, and L. S. Davis, "Viton: An image-based virtual try-on network," in *Proceedings of the IEEE Conference on Computer Vision and Pattern Recognition*, 2018, pp. 7543–7552.
- [5] B. Wang, H. Zheng, X. Liang, Y. Chen, L. Lin, and M. Yang, "Toward characteristic-preserving image-based virtual try-on network," in *Proceedings of the European Conference on Computer Vision (ECCV)*, 2018, pp. 589–604.
- [6] C.-W. Hsieh, C.-Y. Chen, C.-L. Chou, H.-H. Shuai, and W.-H. Cheng, "Fit-me: Image-based virtual try-on with arbitrary poses," in *2019 IEEE International Conference on Image Processing (ICIP)*. IEEE, 2019, pp. 4694–4698.
- [7] N. Zheng, X. Song, Z. Chen, L. Hu, D. Cao, and L. Nie, "Virtually trying on new clothing with arbitrary poses," in *Proceedings of the 27th ACM International Conference on Multimedia*. ACM, 2019, pp. 266–274.
- [8] C.-W. Hsieh, C.-Y. Chen, C.-L. Chou, H.-H. Shuai, J. Liu, and W.-H. Cheng, "Fashionon: Semantic-guided image-based virtual try-on with detailed human and clothing information," in *Proceedings of the 27th ACM International Conference on Multimedia*. ACM, 2019, pp. 275–283.
- [9] F. Sun, J. Guo, Z. Su, and C. Gao, "Image-based virtual try-on network with structural coherence," in *2019 IEEE International Conference on Image Processing (ICIP)*. IEEE, 2019, pp. 519–523.
- [10] Z. Wu, G. Lin, Q. Tao, and J. Cai, "M2e-try on net: Fashion from model to everyone," in *Proceedings of the 27th ACM International Conference on Multimedia*. ACM, 2019, pp. 293–301.
- [11] R. Alp Güler, N. Neverova, and I. Kokkinos, "Densepose: Dense human pose estimation in the wild," in *Proceedings of the IEEE Conference on Computer Vision and Pattern Recognition*, 2018, pp. 7297–7306.
- [12] Z. Cao, T. Simon, S.-E. Wei, and Y. Sheikh, "Realtime multi-person 2d pose estimation using part affinity fields," in *The IEEE Conference on Computer Vision and Pattern Recognition (CVPR)*, 2017.
- [13] X. Liang, L. Lin, W. Yang, P. Luo, J. Huang, and S. Yan, "Clothes co-parsing via joint image segmentation and labeling with application to clothing retrieval," *IEEE Transactions on Multimedia*, vol. 18, no. 6, pp. 1175–1186, 2016.
- [14] K. Gong, X. Liang, D. Zhang, X. Shen, and L. Lin, "Look into person: Self-supervised structure-sensitive learning and a new benchmark for human parsing," in *Proceedings of the IEEE Conference on Computer Vision and Pattern Recognition*, 2017, pp. 932–940.
- [15] A. B. Mabrouk and E. Zagrouba, "Abnormal behavior recognition for intelligent video surveillance systems: A review," *Expert Systems with Applications*, vol. 91, pp. 480–491, 2018.
- [16] R. Zhao, W. Ouyang, and X. Wang, "Unsupervised salience learning for person re-identification," in *Proceedings of the IEEE Conference on Computer Vision and Pattern Recognition*, 2013, pp. 3586–3593.
- [17] Z. Liu, S. Yan, P. Luo, X. Wang, and X. Tang, "Fashion landmark detection in the wild," in *European Conference on Computer Vision*. Springer, 2016, pp. 229–245.

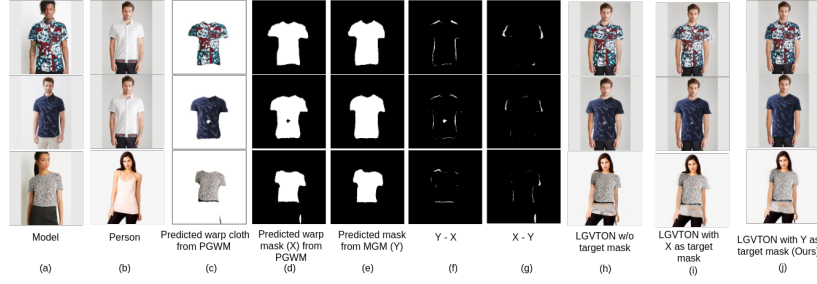


Fig. 12: [Zoom in for details] Effectiveness of target mask generated by our mask generator module (MGM). We notice significant differences (as shown in (f), (g)) between the mask (d) of the predicted warped cloth (c) and the mask (e) predicted by MGM corresponding to the warp cloth (c). (h) shows the final try-on result contains artifacts, when ISM is trained without the target mask. To show the effectiveness of target mask we also show the result where, instead of (e) we give (d) as target mask input to ISM; which is shown in (i). As we observe the artifacts still remain in (i). Whereas, when (e) is given to ISM as target mask, the result (j) improves, e.g., the areas with pixel value 1 in (f) are filled with necessary colour and texture details and those in (g) are replaced with background details resulting in a better VTON result. Note that the hole in the warp cloth in row 2 is not due to warping fault. This is due to the inaccurate human parsing. However LGVTON handles this also.

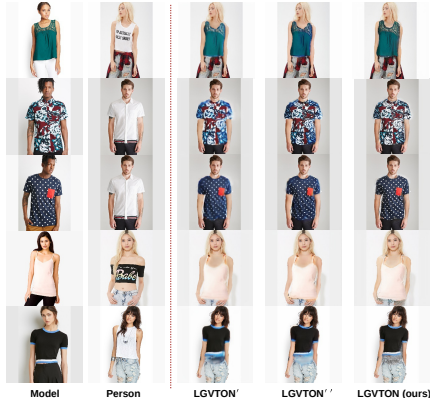


Fig. 13: [Better viewed in electronic version and zoomed in] Effectiveness of different losses during training the Image Synthesizer module (ISM) of LGVTON. (1) LGVTON' - ISM trained with DSSIM loss only (non GAN variant), (2) LGVTON'' - ISM as cGAN trained with DSSIM loss (for generator) and adversarial loss, (3) LGVTON - similar to (2) but generator is trained with DSSIM and VGG perceptual loss both. It can be observed that (1) it produces blur output. Although in presence of adv. loss the blurriness of the output is reduced resulting in a better quality output, but when trained with all the 3 losses i.e., DSSIM, adversarial, perceptual (LGVTON) the quality of the result looks much better with improved cloth details and better reconstructed human skin colour etc.

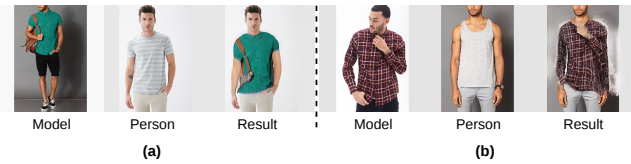


Fig. 14: Failure cases of LGVTON. (a) Incorrectly segmented model cloth results in poor vton output. As here the model's hand and bag strap are segmented as cloth incorrectly and it affects our result. (b) The proposed method of warping can not unfold the sleeves of the cloth from cross folded position. As seen here the model's cloth sleeve on his left hand is cross folded. Which could not be unfolded in the result to warp according to person pose.

Pattern Recognition, 2018, pp. 4271–4280.

- [19] D. Anguelov, P. Srinivasan, D. Koller, S. Thrun, J. Rodgers, and J. Davis, "Scape: shape completion and animation of people," *ACM Trans. Graph*, vol. 24, pp. 408–416, 2005.
- [20] A. Raj, P. Sangkloy, H. Chang, J. Hays, D. Ceylan, and J. Lu, "Swapnet: Image based garment transfer," in *Computer Vision - ECCV 2018 - 15th European Conference, Munich, Germany, September 8-14, 2018, Proceedings, Part XII*, 2018, pp. 679–695.
- [21] M. Zanfir, A.-I. Popa, A. Zanfir, and C. Sminchisescu, "Human appearance transfer," in *The IEEE Conference on Computer Vision and Pattern Recognition (CVPR)*, June 2018.
- [22] M. Mirza and S. Osindero, "Conditional generative adversarial nets," *arXiv preprint arXiv:1411.1784*, 2014.
- [23] J. Duchon, "Splines minimizing rotation-invariant semi-norms in sobolev spaces," in *Constructive theory of functions of several variables*. Springer, 1977, pp. 85–100.
- [24] R. Sprengel, K. Rohr, and H. S. Stiehl, "Thin-plate spline approximation for image registration," in *Proceedings of 18th Annual International Conference of the IEEE Engineering in Medicine and Biology Society*, vol. 3. IEEE, 1996, pp. 1190–1191.
- [25] G. Donato and S. Belongie, "Approximate thin plate spline mappings," in *European conference on computer vision*. Springer, 2002, pp. 21–31.
- [26] I. Goodfellow, J. Pouget-Abadie, M. Mirza, B. Xu, D. Warde-Farley, S. Ozair, A. Courville, and Y. Bengio, "Generative adversarial nets," in *Advances in neural information processing systems*, 2014, pp. 2672–2680.
- [27] A. Newell, K. Yang, and J. Deng, "Stacked hourglass networks for human pose estimation," in *European conference on computer vision*. Springer, 2016, pp. 483–499.
- [28] P. Isola, J.-Y. Zhu, T. Zhou, and A. A. Efros, "Image-to-image translation with conditional adversarial networks," in *Proceedings of the IEEE conference on computer vision and pattern recognition*, 2017, pp. 1125–1134.
- [29] W. Xian, P. Sangkloy, V. Agrawal, A. Raj, J. Lu, C. Fang, F. Yu, and J. Hays, "Texturagan: Controlling deep image synthesis with texture patches," in *Proceedings of the IEEE Conference on Computer Vision and Pattern Recognition*, 2018, pp. 8456–8465.
- [30] J. Johnson, A. Alahi, and L. Fei-Fei, "Perceptual losses for real-time style transfer and super-resolution," in *European conference on computer vision*. Springer, 2016, pp. 694–711.
- [31] Z. Wang, A. C. Bovik, H. R. Sheikh, E. P. Simoncelli *et al.*, "Image quality assessment: from error visibility to structural similarity," *IEEE transactions on image processing*, vol. 13, no. 4, pp. 600–612, 2004.
- [32] S. Kubo, Y. Iwasawa, and Y. Matsuo, "Generative adversarial network-based virtual try-on with clothing region," 2018.
- [33] Z. Liu, P. Luo, S. Qiu, X. Wang, and X. Tang, "Deepfashion: Powering robust clothes recognition and retrieval with rich annotations," in *Proceedings of the IEEE conference on computer vision and pattern recognition*, 2016, pp. 1096–1104.
- [34] T. Salimans, I. Goodfellow, W. Zaremba, V. Cheung, A. Radford, and X. Chen, "Improved techniques for training gans," in *Advances in neural information processing systems*, 2016, pp. 2234–2242.
- [35] M. Heusel, H. Ramsauer, T. Unterthiner, B. Nessler, and S. Hochreiter, "Gans trained by a two time-scale update rule converge to a local nash

[18] W. Wang, Y. Xu, J. Shen, and S.-C. Zhu, "Attentive fashion grammar network for fashion landmark detection and clothing category classification," in *Proceedings of the IEEE Conference on Computer Vision and*

- equilibrium,” in *Advances in Neural Information Processing Systems*, 2017, pp. 6626–6637.
- [36] C. Szegedy, V. Vanhoucke, S. Ioffe, J. Shlens, and Z. Wojna, “Rethinking the inception architecture for computer vision,” in *Proceedings of the IEEE conference on computer vision and pattern recognition*, 2016, pp. 2818–2826.
- [37] J. Deng, W. Dong, R. Socher, L.-J. Li, K. Li, and L. Fei-Fei, “ImageNet: A Large-Scale Hierarchical Image Database,” in *CVPR09*, 2009.